Journal of Rehabilitation in Civil Engineering 5-2 (2017) 49-65

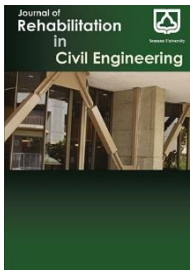

Journal homepage: http://civiljournal.semnan.ac.ir/

Experimental and Numerical Investigation of Two Fixed-End RC Beams Strengthened With CFRP Bars in NSM Method

M. Mohammadian[1] and M.K. Sharbatdar[2*]
1. M.Sc., Structural Engineering, Roshde Danesh Institute of Education, Semnan, Iran.
2. Associate Professor, Faculty of Civil Engineering, Semnan University, Semnan, Iran.

Corresponding author: *msharbatdar@semnan.ac.ir*

ARTICLE INFO

Article history:
Received: 24 October 2015
Accepted: 03 April 2017

Keywords:
NSM Method,
FRP Bars,
RC Beam,
Flexural Capacity,
Strengthening.

ABSTRACT

Fiber-reinforced polymer (FRP) material is currently being produced in different configurations and widely applied to strengthening and retrofit concrete structures and bridges. It is also possible to apply other strengthening methods without changing the appearance or the dimensions of the structure. Near Surface Mounted (NSM) is a recent strengthening method using CFRP bars (rods or laminate strips) bonded into pre-cut grooves applied to the concrete cover of the elements to be strengthened. These FRP bars can help increase the flexural and shear capacity of existing concrete members as well. This article aims to present the experimental and numerical results gained separately from un-strengthened and strengthened beams under bending loading. In the experimental part, two large-scale fixed-end support reinforced concrete beams of the same size, and reinforcement characteristic was designed, constructed, and tested under one point concentrated loading system. The first specimen used as a control specimen while the second served as the strengthened applying NSM method with a new proposed hand-made CFRP Bar in the laboratory. Moreover; an extra analytical work was carried out using calibration of the analytical models as per the obtained experimental test results. The results and Photographs taken at the selected stages of loading are indicative of the fact that NSM method with FRP bars can be effectively applied to the existing structures in order to increase their flexural capacity, change their crack pattern and decrease final deflection.

1. Introduction

A large number of existing buildings and bridges are in need of strengthening or retrofitting due to factors such as deterioration, construction or design faults, additional load, or functional change. Fiber

DOI: 10.22075/jrce.2017.974.1118

Reinforced Polymer (FRP) reinforcements have been recently used broadly as an alternative reinforcement material in place of steel for new construction as well as for strengthening and repair of the existing concrete structures. To improve utilization of the FRP materials, near-surface mounted (NSM) reinforcement was recently introduced as a promising technique for the strengthening of reinforced concrete members. Application of NSM FRP reinforcement does not require surface preparation work and requires minimal installation time and cost after cutting the groove compared to the externally bonded reinforcing (EBR) technique. In this new technique, FRP bars or strips are embedded applying a suitable binding agent (epoxy paste or cement grout) in grooves cut in the cover of a concrete member, as near-surfaced mounted (NSM) reinforcement for flexural or shear strengthening purposes. Examples of NSM steel rebars used in Europe to strengthen RC structures date back to the 1950s. The advantages of FRP versus steel as NSM reinforcement are the better resistance to corrosion, increased ease and speed of installation due to its lightweight, and a reduced groove size attributable to the higher tensile strength and better corrosion resistance of FRP. Compared to externally bonded FRP reinforcement, the NSM system has a number of advantages such as (a) the amount of site installation work may be reduced, so surface preparation is no longer required (e.g., plaster removal is not necessary; irregularities of the concrete surface can be more easily accommodated; removal of the weak laitance layer on the concrete surface is no longer required); (b) NSM reinforcement is less prone to debonding from the concrete substrate; (c) NSM bars can be more easily anchored into the adjacent members to prevent debonding failures; this feature is particularly attractive in the flexural strengthening of beams and columns in rigidly-jointed frames, where the maximum moments typically occurred at the ends of the member; (d) NSM reinforcement can be more easily pre-stressed; (e) NSM bars are protected by the concrete cover and so are less exposed to accidental impacts and mechanical damages, fire, and vandalism; this aspect makes this technology particularly appropriate for the strengthening of negative moment regions of beams/slabs; (f) the aesthetic of the strengthened structure is virtually the same. As a result of the above advantages, the NSM FRP method is in many cases superior to the externally bonded FRP method or can be used in combination with it, provided that the cover of the member is sufficiently thick for grooves of a desirable size to be contributed. Barros and Dias [1] tested beams with different sizes without internal stirrups. Some of these beams were strengthened with NSM CFRP strips at the different inclinations, while the rest were strengthened with equivalent amounts of externally bonded FRP shear reinforcement. The reported strength increases ranged from 22% to 77%, and were in all cases larger than those obtained with externally bonded FRP and some of the beams were believed to have failed in bending. Almost all test results indicated that the NSM technique improved the ultimate load and the load at the yielding of steel reinforcement, as well as the post-cracking stiffness (De Lorenzis and Nanni 2007) [2]. Asplund (1949) demonstrated tests on concrete beams strengthened with NSM steel bars grouted into diamond-sawed grooves filled with cement mortar and compared their behavior with that of conventional concrete beams reinforced with steel bars. Identical behavior for both sets of

specimens was observed. The same technique was applied in strengthening a reinforced concrete bridge deck in Sweden that experienced excessive settlement of the negative moment reinforcement during construction so that the negative moment capacity is required to be increased [3]. Nordin and Täljsten tested fifteen beams with a length of 4m that Strengthened with Prestressed Near Surface Mounted CFRP. The beam strengthened with prestressed NSM CFRP rods displayed about a 100 and 37% increase in the cracking and yielding load, respectively, compared with the beam strengthened with nonprestressed NSM CFRP rods. The tests persuade that the ultimate load at failure of prestressed beams was also higher, and the prestressed beams exhibited a higher first-crack load and smaller midpoint [4]. Based on the available experimental evidence reported in previous studies, the possible flexural failure modes of strengthened beams with NSM FRP reinforcement are different such as bar–epoxy interfacial de-bonding, concrete cover separation, bar end cover separation, localized cover separation, flexural crack-induced cover separation, beam edge cover separation, and epoxy–concrete interfacial de-bonding. The application of NSM FRP reinforcement is also effective in improving the shear capacity of RC beams.

De Lorenzis and Nanni investigated the structural performance of simply supported reinforced concrete beams strengthened with near-surface mounted GFRP and CFRP rods. Both flexural and shear strengthening were examined. Test results revealed that the use of near-surface mounted FRP rods is an effective technique to enhance flexural and shear capacity of reinforced concrete beams. The beams strengthened in bending exhibited an increase in capacity ranging from 26 to 44% over the control beam. For the beams strengthened in shear, an increase in capacity as high as 106% was achieved [5]. Hassan and Rizkalla investigated the feasibility of applying different strengthening techniques as well as different types of FRP for strengthening concrete structures. Large-scale models of a prestressed concrete bridge were tested up to failure. Test results indicated that the efficiency of near-surface mounted CFRP strips were three times better than externally bonded strips [6]. De Lorenzis and Nanni found that the maximum tensile strain in the CFRP and GFRP bars applied as NSM reinforcement did not exceed 33% and 60% of rupture strain of the bar at failure, respectively [7]. Carolin examined a series of concrete beams strengthened with near-surface mounted CFRP strips. Test results demonstrated the effectiveness of the near-surface mounting technique compared to the externally bonded technique. Carolin recommended replacing the epoxy, used in bonding the strips to the surrounding concrete, with cement mortar to improve the work environment on-site [8]. Jalali and Sharbatdar evaluated the effectiveness of NSM technique using innovative, manually made FRP rods (MMFRP) for shear strengthening of RC beams. The strengthened specimens displayed between 25% and 48% over the control beam [9]. Pursuant to Tanarslan study on the shear capacity of strengthened RC beam in NSM method, an increase of minimum 57% and maximum 112% in shear capacity in comparison to the control beam was obtained [10]. Experimental research has indicated that the NSM technique has significant potential for increasing the load-carrying of continuous RC slabs [11].

2. Research Significant

To assess the effectiveness of NSM strengthening techniques and increase the flexural resistance of RC beams, two experimental specimens with two fixed-ended supports were selected. To simulate a real strengthening situation, flexural beams had a limited amount of longitudinal flexural reinforcement.

In order to investigate the numerical behavior of beams, both experimental specimens were designed and analyzed in the finite element program (ABAQUS). C3D8R element was applied for meshing of concrete. Steel and FRP bar was modeled by T3D2 element. Finally, the numerical and experimental results were compared to each other, and after the calibration program, the variables such as the effect of FRP bars cross area on strengthened beam were examined in ABAQUS.

3. Experimental Work

3.1. Specimen Details and Material Properties

Geometry, reinforcement arrangements, loading, and supporting conditions of the flexural beams are represented in Fig 1. The two-end fixed rectangular beams had an overall length of 242 cm, the clear span of 182 cm, the depth of 20 cm and a clear width of 30 cm. The average compression concrete strength of cylinder specimens was 46 MPa. The tensile and compressive steel reinforcement was composed of three 10 mm diameters bars at the top and three at the bottom. The yielding and ultimate stresses of these steel bars were about 385 and 560 MPa, respectively. Shear reinforcement was 8 mm diameter, uniformly spaced at 70 mm. Shear reinforcement was selected to prevent shear failure prior to bending failure for beams. The yielding and ultimate stresses of shear steel bars were about 340 and 490 MPa, respectively. The beams were fixed at two ends with columns connected to each beam. Each supported column contained eight 16 mm diameters bars. The two-end fixed beams were joined to laboratory rigid frame with 8 bolt in each connected column and then loaded under concentrated load.

3.2. Strengthening System

BF1 specimen was examined as a control un-strengthened specimen. The second specimen, BF2, was strengthened with applying NSM CFRP bars with one FRP bar at each tension area side, at the top of the end support in the negative moment's region and at the bottom of the middle of the beam for the positive moment as well. The cross-section was about 8 mm2 for each FRP bar. The BF2 specimen was strengthened with embedment lengths of about 90 percent of the beam total length (182 cm) at the tensile part at the bottom and both tensile parts at the top near the supports. The size of the groove was 20*20mm that was filled with epoxy C330 made by Sireg Corporation. This strengthening is illustrated in Fig 2.

A new type of CFRP bar was proposed in this study, the CFRP bars were manually made in the laboratory and were hooked at the end for anchoring in concrete. The CFRP bars had a circular cross section and made of three-ingredient; i) CFRP sheet, ii) epoxy resin and iii) wooden bar. A high strength unidirectional carbon sheet with 0.11 mm nominal fiber thickness (Table 1), impregnated in situ with epoxy resin by the wet lay-up technique. The nominal fiber content was 60% by volume. The manufacturer's values of tensile strength and elastic modulus of CFRP sheets was equal to 3550 MPa and 235 GPa, respectively, with an ultimate tensile strain of 1.5%.

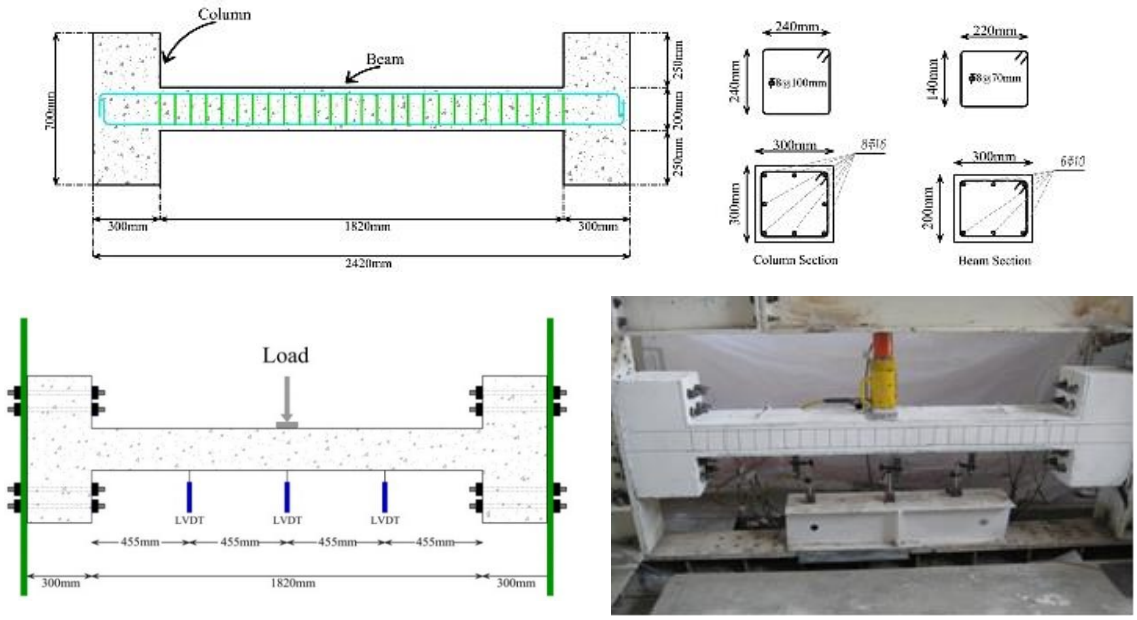

Fig. 1. Experimental specimens Details.

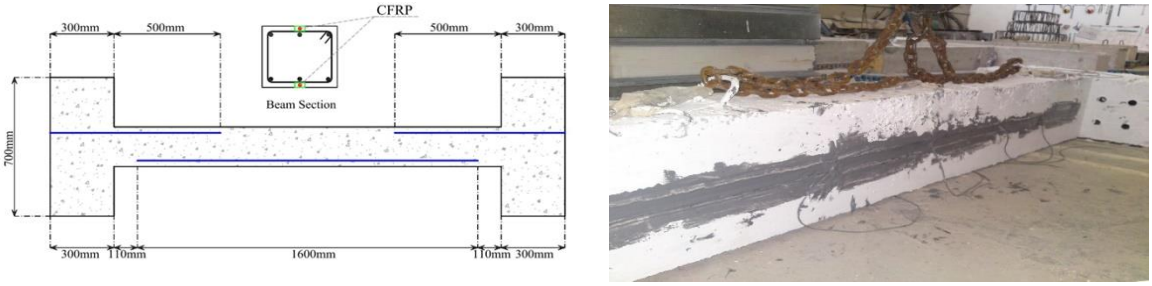

Fig. 2. Location of CFRP bars at the strengthened specimen.

Table 1. Mechanical Properties of Epoxy used in Strengthening.

Adhesive	**Application**	**Tension strength** (MPa)	**Modulus of Elasticity** (GPa)	**Density** (Kg/l)	**Ultimate strain** (%)	**Maximum using Time** (Minutes)	**Curing time** (Day)
Epoxy G400	CFRP Bar	50	1600	1.115	3%	75	5
Epoxy C330	NSM	30	----	1.350	1.6%	60	5

The adhesive was epoxy G400 made in Sireg Corporation. The fabrication process of hand-made CFRP bars is displayed in Fig 3. The mechanical properties of FRP bars and adhesive presented in Tables 2 and 3. Mechanical properties of FRP bars were established through tension test with the procedure specified in Canadian standard S806. Stress-strain relationship of FRP bars is indicated in Fig. 4, indicating that CFRP bars have linear elastic behavior.

Table 2. Mechanical properties of handmade CFRP bars.

FRP Cross Area (mm^2)	Modulus of Elasticity (GPa)	Tension strength (MPa)	Strain
8	225	2150	0.01

Table 3. Mechanical properties of FRP fibers were used in making handmade CFRP bars.

Product	Fiber	Modulus of Elasticity (GPa)	Tension Strength (MPa)	Ultimate strain (%)	Thickness (mm)
YC-N200	High Strength Carbon	235	3550	1.5	0.11

Fig. 3. Making the process of hand-made CFRP bars.

3.3. Instrumentation

Prior to casting the beams, strain gauges were attached at the critical positions on the steel reinforcement and FRP bars. Strain gauges were also attached to all concrete beams at the mid-span, to measure the concrete strain during loading. The beams were instrumented with three LVDTs one in the mid-span and two at the 1/4 length of the beam, to monitor the maximum and average deflections as depicted in Fig 1. The load was applied to each beam at a rate of 5 kN/step by means of the hydraulic jacks. Displacements, strains, and loads were all recorded by an electronic data logger system with a 1-Hz sampling rate.

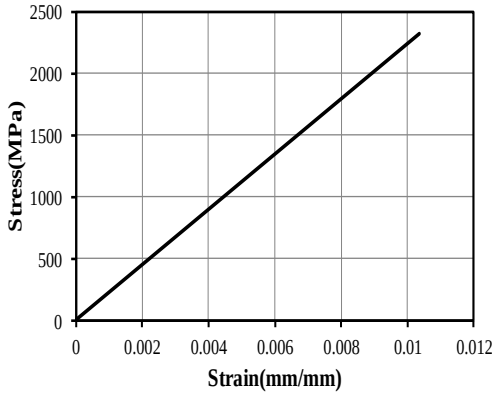

Fig. 4. Stress-strain curve of hand made FRP bars.

4. Test Result and Discussion

Test observations and failure process are indicated in Fig. 5 and also the test Load-Displacement curves are given in Fig 6. The first crack in un-strengthened BF1 specimen was happened at the load 50 kN with corresponding deflection 1.77 mm. The bottom tension-steel bars were yielded at the load 111 kN and deflection 4.92 mm and the top tension-steel bars at the fixed support were yielded at the load 150 kN and deflection 7.50 mm. The final load amount of capacity was 230kN and 22.7 mm deflection. The flexural failure mode was observed, as

shown in Fig 5-a, much more cracks were observed in tension zones of concrete and consequently crushed in the compression parts of the beam at the end of testing. The first crack in strengthened BF2 specimen was happened at the load 40 kN with corresponding deflection 1.39 mm. Bottom tension-steel bars were yielded at the load 87.5 kN and deflection 4.29 mm and the top tension-steel bars were yielded at the load 160 kN and deflection 8.4 mm. The final load amount of capacity was 260 kN with 19.6 mm deflection. These results are aligned in Table 1. As shown

in Fig 5-b, most of the cracks at the tension zones were flexural mode. The FRP bar rupturing and concrete crushing was observed at the end of the test. The initially required cross-section of mounted bars was calculated based on the design code nominal moment capacity of the specimen equal to (M_n). M_n was assumed to be equal to 15 kN.m for this section based on CSA (Canadian design code), so consequently means that the maximum expected nominal load capacity should be equal to 65 kN. According to Fig 6, the unstrengthened specimen BF1 tolerated the maximum capacity equal to approximately 230 kN that was almost three and half time higher than that of 65 kN as nominal load capacity, as a result of two fixed-end with three degrees uncertainly and moment redistribution. Consequently, even though some FRP bars were applied to increase the flexural capacity, but only about %15 increase was observed. It seemed that the mounted bars with about 8 mm^2 cross-section, were not sufficient to have a significant increase of capacity and indicating NSM method more efficiently, so the FRP bars stresses in BF2 specimen were increased very soon and they were ruptured around strain 0.011 and could not the BF2 specimen capacity much more effectively. Thus, both specimens had about %15 difference in capacity with different ductility. Load-strain behavior of top and bottom steel and FRP bars are illustrated in Figures 7, 8, 9.

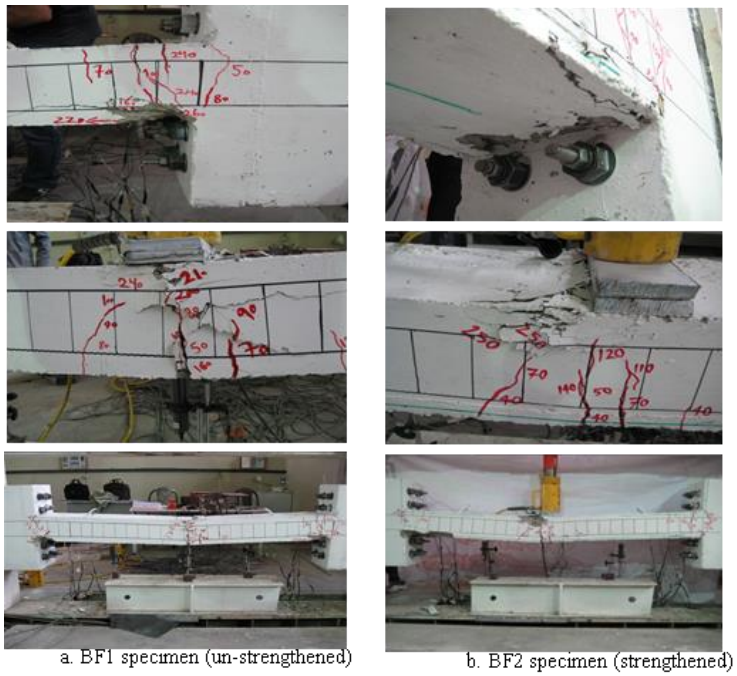

a. BF1 specimen (un-strengthened) b. BF2 specimen (strengthened)

Fig. 5. Flexural failure in two fixed end specimen.

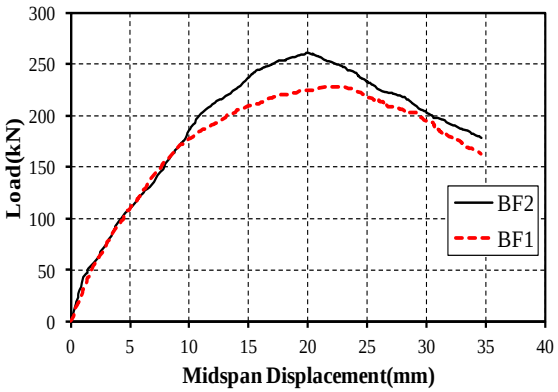

Fig. 6. Midspan load-deflection behavior.

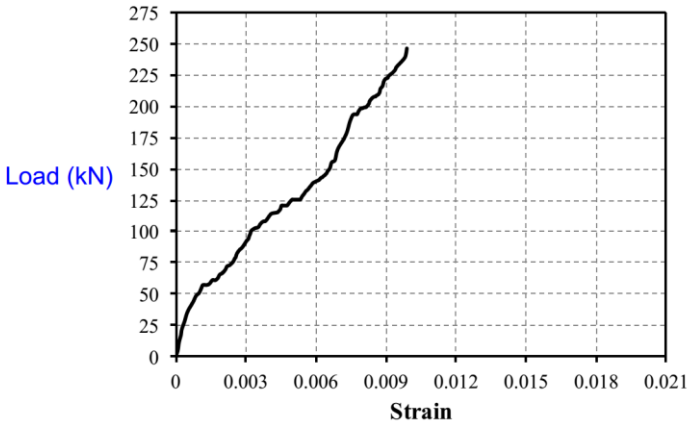

Fig. 7. Load-strain behavior of FRP bars at BF2 strengthened specimen.

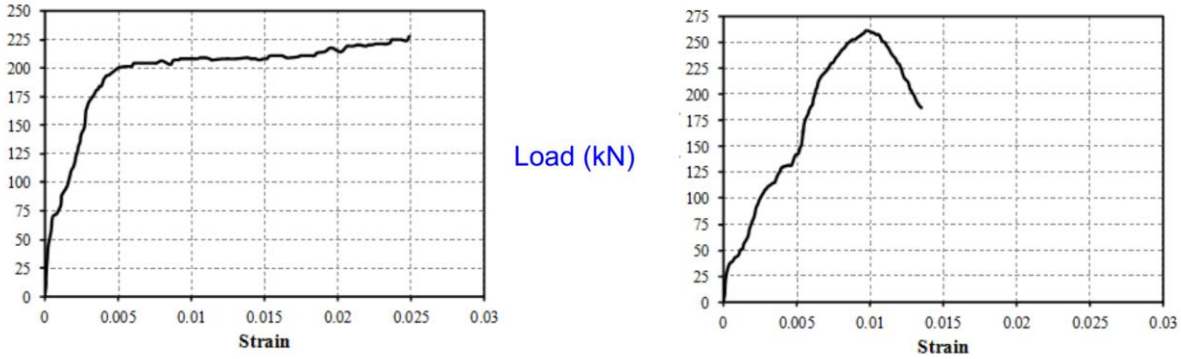

a. BF1 b. BF2

Fig. 8. Load-strain behavior of tensile steel in a positive moment.

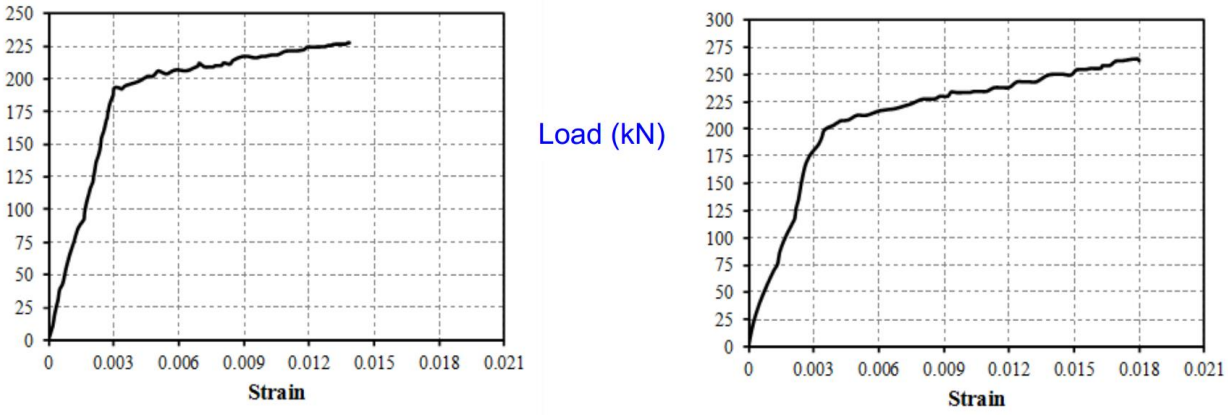

a. BF1 b. BF2

Fig. 9. Load-strain behavior of tensile steel in negative moment.

5. Numerical Modeling and Analysis of Experimental Results

The experimental specimen design, analysis, and calibration in the finite element program, ABAQUS is presented in this section. The properties of extra analytical specimens were exactly similar to experimental specimen such as the size of the RC beam, steel and FRP bars, and material properties. The numerical modeling of the specimen is depicted in Fig 10. The final load capacity and corresponding deflection at the failure of BF1 specimen were 252 kN and 37mm respectively, and those For BF2 specimen were 263.3 kN and 28.22mm respectively. The expanse of cracks in specimens is shown in Fig 11, close to crack pattern in Fig5. The comparison of the numerical and experimental results of both specimens are presented in Fig 12 and aligned in Table 4. There is a good agreement between both numerical and experimental load-deflection curves with little difference. In order to calculate the ductility factor of specimens, the displacement at the yielding, Δ_Y , and failure point, Δ_U , should be calculated and presented in Table 4. The deflection curves of both specimens in different loads are illustrated in Fig 13.

Table 4. Experimental and Numerical Results of specimens testing.

Beam	EXPERIMENTAL								NUMERICAL		
	P_{cr} (kN)	Δ_{cr} (mm)	P_Y (kN)	Δ_Y (mm)	P_U (kN)	Δ_{U1} (mm)	Δ_{U2} (mm)	μ	P_U (kN)	Δ_U (mm)	Failure Mode
BF1	50	1.77	150	7.5	230	22.7	31.1	4.13	252	37	Flexural Failure
BF2	40	1.39	160	8.4	260	19.6	28.8	3.76	263.3	28.22	Flexural Failure

P_{cr} : Cracking Load — Δ_{cr} : Midspan Deflection at Cracking Load

P_Y : Yielding Load — Δ_Y : Midspan Deflection at Yielding Load

P_U : Ultimate Failure Load — Δ_{U1} : Midspan Deflection at real Failure point.

$\mu = \frac{\Delta_{U2}}{\Delta_y}$ (Ductility) — Δ_{U2} : Midspan Deflection at %20 degradation point after ultimate load.

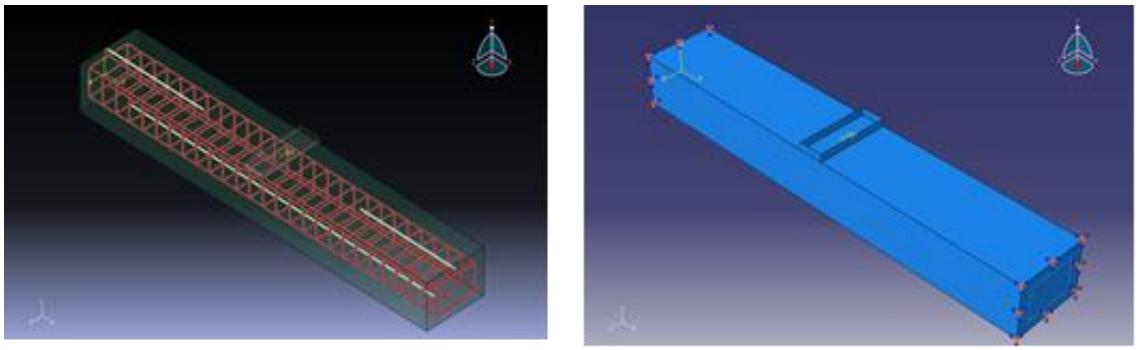

Fig. 10. Numerical specimen in finite element program.

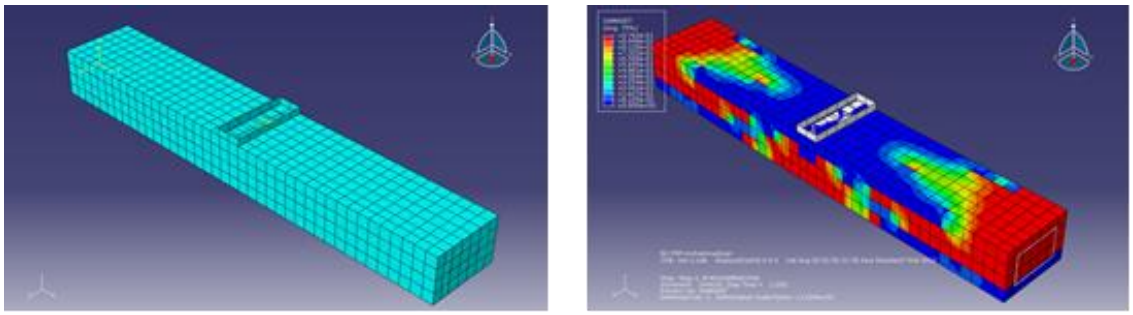

Fig. 4. Mesh modeling and Expanse of cracks in specimens.

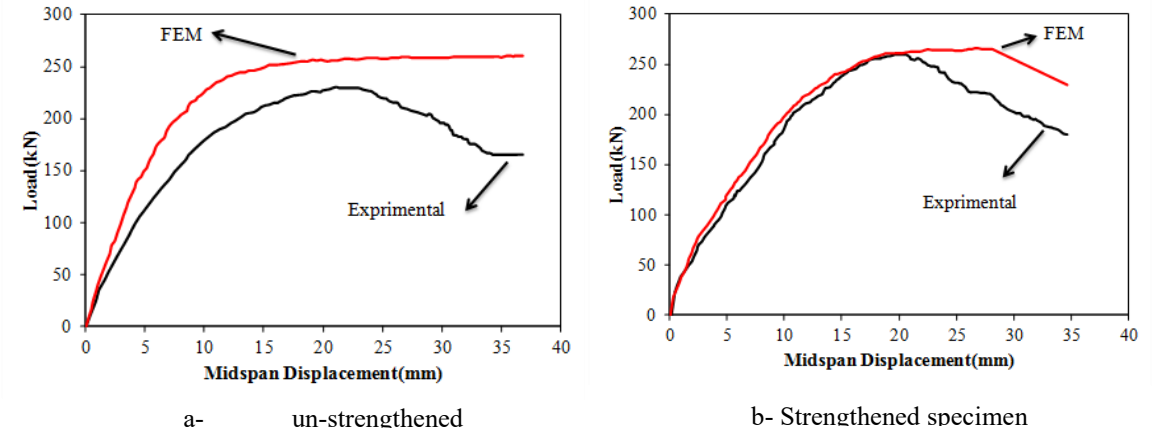

a- un-strengthened b- Strengthened specimen

Fig. 5. Mid-Span Load-Deflection behavior of experimental and numerical specimens.

6. Numerical Variables Investigation

Given the elaboration depicted in the experimental specimen of the previous section, numerical analysis was separately investigated applying two diverse variables, the number and cross-area of FRP bars and concrete compression strength, so the numerical specimens were classified at the two different groups. At the first group named B45-F, concrete compression strength was 45 MPa the same as the experimental specimen, and in the second group named B25-F, concrete compression strength was 25 MPa. The dimensions of beams and steel properties were companion to the experimental specimens. In each group, 10 mm diameter FRP bars were used as 1, 2, and 3 bars in the tensions zone portrayed in Fig 14. In order to consider probable debonding

of FRP Bars prior to the final crushing of concrete, based on the previous research [12], the FRP ultimate tension stress was assumed to be 1800 MPa. Numerical specimen details were similar to Fig1. Table 5 indicates specimens characteristics.

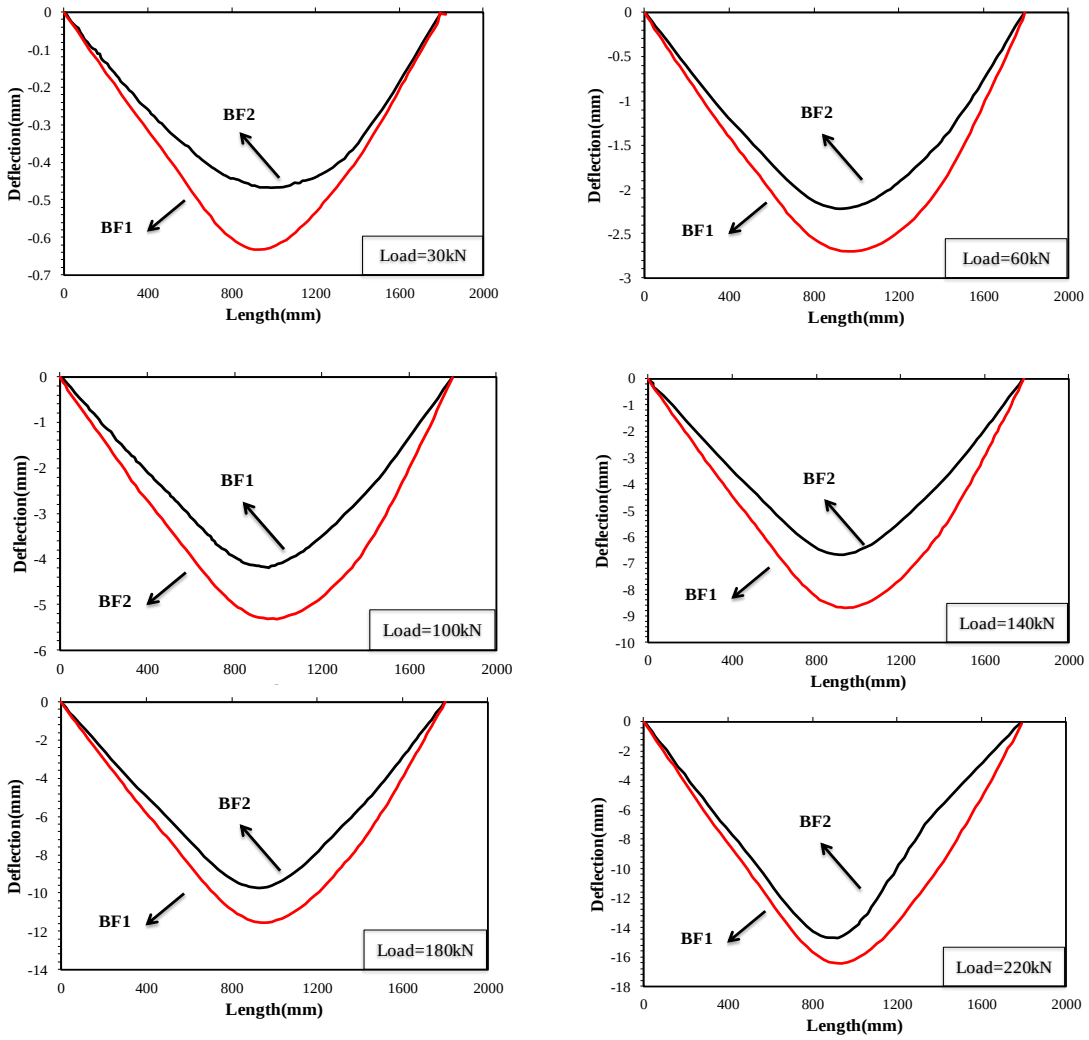

Fig. 13. Deflection curves of experimental specimens at different loads

Table 5. Specimen designed in finite element program.

The number and of FRP bars	Concrete compression strength (MPa)	Specimen	
_____	45	B45-F0	1
1	45	B45-F1	2
2	45	B45-F2	3
3	45	B45-F3	4
_____	25	B25-F0	5
1	25	B25-F1	6
2	25	B25-F2	7
3	25	B25-F3	8

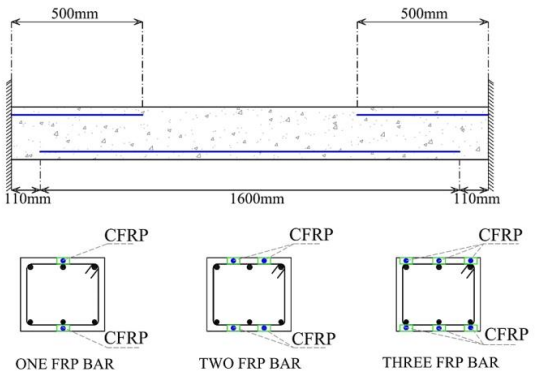

Fig. 6. Location of CFRP bars in numerical specimens.

- **B45 Group**

B45-F0 concrete compression strength specimen with 45 MPa didn't have any FRP bars and applied as a reference beam for investigating of the strengthened specimen. The first crack occurred at 48 kN load with 1.4mm midspan deflection. Changing the slope of curved at 130 kN load and 4mm deflection indicated the yielding of tension steel. By increasing loading, longitudinal steels were reached to hardening step and finally as a result to decreasing neutral chord and so increasing compressive stress in compressive concrete; the beam was reached at the ultimate load equal to 252 kN and the deflection equal to 37 mm. According to Fig 13, the B45-F1 specimen had one FRP bar at each tension zone for positive and negative moments. The first crack occurred at 50 kN load with 1 mm midspan deflection. Modifying the slop of curved at 180 kN load and 5mm deflection indicated the yielding of tension steel. The behavior of this beam was a companion to reference beam up to yielding of steel Bar, B45-F0, after that point due to the existence of FRP; the ultimate capacity was increased. Finally, debonding in FRP and crushing of concrete occurred and beam failed at the ultimate load equal to 281.02 kN and the corresponding deflection equal to 34.99 mm. The properties of B45-F2 specimen was a companion to B45-F1 specimen but had two FRP bars at each tension zone of beam. The first crack occurred at 52 kN load with 0.9 mm midspan deflection. 185 kN load and 4.4mm deflection indicated the yielding of tension steel and finally at the end of analysis debonding of FRP occurred and beam failed at the load equal to 311.8 kN and the deflection equal to 32.32. B45-F3 specimen had three FRP bars at each tension zone of beam depicted in Fig 15. with 50 kN load with 0.8 mm midspan deflection. 193 kN load and 3.8mm deflection were indicated the yielding of tension steel. In this specimen, debonding in FRP did not occur, and finally, the beam failed at the load equal to 324 kN and the deflection equal to 30.98 mm due to concrete crushing. Load-deflection curve of beams B45-F group is compared with each other In Fig 16. It was obvious that strengthening with FRP caused significant increasing in capacity and decreasing in the ductility. B45-F1, B45-F2 and B45-F3 specimens had increasing beam capacity about 11.5%, 23.5% and 28.5% respectively and also decreasing about 5.7%, 14.4% and 19.5% midspan deflection compare to reference specimen, B45-F0, shown in Table 6.

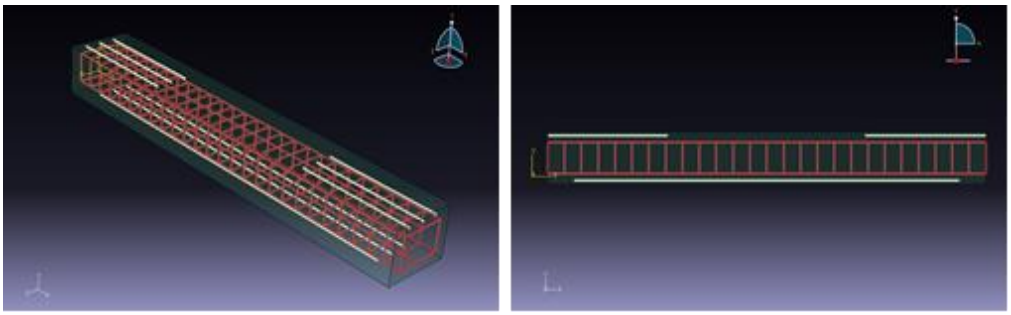

Fig. 7. Location of FRP bars in B45-F3 specimen.

Table 6. Numerical results of B45-F Group.

Specimen	P_u *(kN)*	***Increasing in capacity*** *(%)*	Δ_u *(mm)*	***Decreasing midspan deflection*** *(%)*	$\frac{A_F}{A_S}$ *(%)*
B45-F0	252	———	37	———	———
B45-F1	281.02	%11.5	34.99	%5.7	%33
B45-F2	311.8	%23.5	32.32	%14.4	%66
B45-F3	324	%28.5	30.96	%19.5	%100

B45-F2 specimen in juxtapose with the other specimens had more increasing the amount of capacity, although B45-F3 specimen had more FRP bars, all FRP capacity was not cached prior to debonding due to earlier compressive concrete crushing. In consonance with numerical analysis, the balance FRP area was equal to A_{Fb}= 4.21 cm2. In B45-F1 and B45-F2 specimens, cross-area of FRP bars was less than A_{Fb}, so FRP bars were reached to their debonding stress. Bar area in B45-F3 was more than A_{Fb}; thus concrete was crushed in compression zone and beam collapsed prior to FRP debonding. On the other hand, increasing the cross area of FRP until certain amount, caused an increase in the amount of capacity and decreasing ductility indicated in Fig 17.

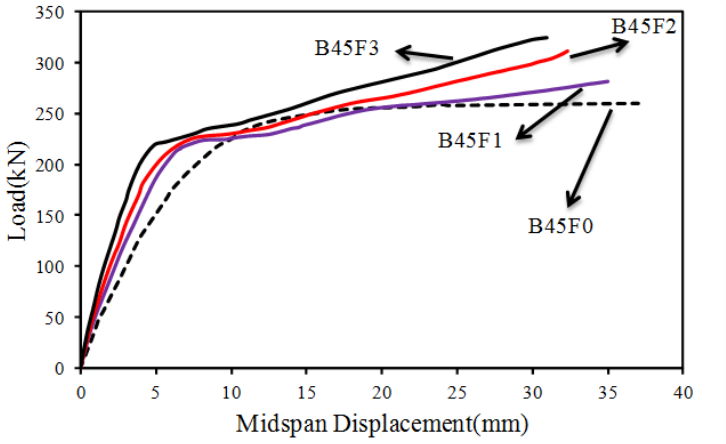

Fig. 8. Load-deflection curves of B45-F group

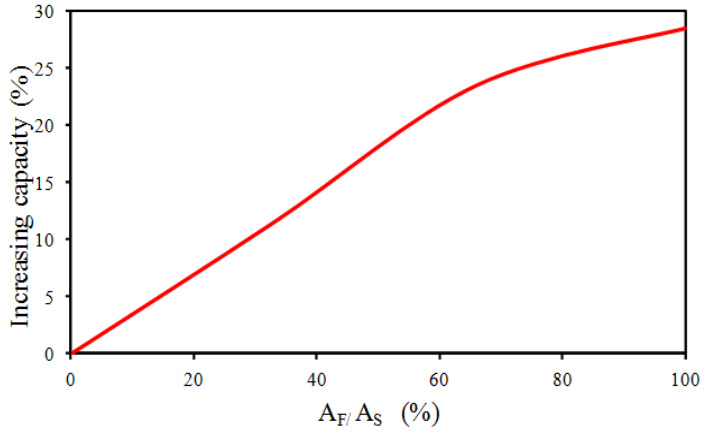

Fig. 9. Effect of cross-area of FRP bars on specimen capacity for F'c=45 MPa

- **B25 Group**

in order to consider the concrete compression strength effect on strengthening, the new group specimens were analyzed again with a concrete compression strength of 25 MPa. The other properties of B25-F group were exactly similar to B25-F group. B25-F0 specimen didn't have any FRP bars and applied as a reference beam for investigating of the strengthened specimen. The first crack occurred at 33 kN load with 0.8mm midspan deflection, and finally, due to decreasing neutral chord and crushing of compression concrete, the beam was failed at the load equal to 225.1 kN and the deflection equal to 43.03 mm. B25-F1 specimen had one FRP bar at each tension zone of the positive and negative moment. Its first crack occurred at 33 kN load with 0.78 mm midspan deflection. Till yielding of tension steel, the behavior of this beam was a companion to reference beam, B25-F0, and then the ultimate amount of capacity has increased as a result of the existence of FRP. Finally, the debonding in FRP occurred and beam failed at the load in FRP occurred and beam failed at the load equal to 267.8 kN and the deflection equal to 38.63 mm. The properties of B25-F2 specimen was a companion to B25-F1 specimen but had two FRP bars at each tension zone of beam. The first crack occurred at 35 kN load with 0.75 mm midspan deflection. Finally, the debonding in FRP didn't occur because of crushing concrete in compression zones; hence,the beam failed at the load equal to 283.2 kN and the deflection equal to 31.2 mm. B25-F3 specimen had three FRP bars at each tension zone of beam. The first crack occurred at 37 kN load with 0.7 mm midspan deflection. As presented in Fig 18, In this specimen, the debonding in FRP didn't occur and finally because of crushing concrete in compression zones, the beam failed at the load equal to 290.1 kN and the deflection equal to 29.58 mm.

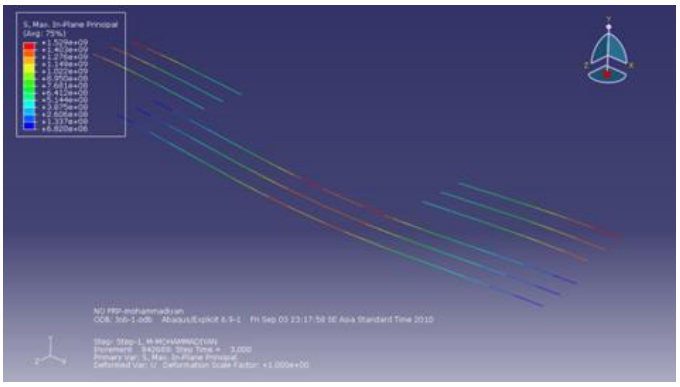

Fig. 10. Not Arriving FRP bars to debonding stress in B25-F3 specimen.

Load-deflection curve of B25-F group is compared together in Fig 19. It was obvious that strengthening with FRP cause increasing in capacity and decreasing in ductility. B25-F1, B25-F2 and B25-F3 specimen capacities were increased about 19%, 25.8% and 28.8% respectively and midspan deflection were decreased about 11.4%, 38.7% and 45.4% rather than references specimen ,B25-F0, illustrated in Table 7. The cross-section of FRP bar effect on specimen capacity for concrete with compressive strength of 25 MPa is shown in Fig20, and it is indicating that increasing of capacity doesn't have liner relationship with increasing of FRP Bar area percentage. Comparison between Table 6 and 7 indicates that %40 decreasing of concrete compression strength caused averagely %10 decreasing of capacity with same FRP Bar area, but revealing different effect on deflection mostly on the specimen with less FRP Bars.

Table 7. Analysis result of B25-F group.

Specimen	P_u *(kN)*	***Increasing in capacity*** *(%)*	Δ_u *(mm)*	***Decreasing midspan deflection (%)***	$\frac{A_F}{A_S}$ *(%)*
B25-F0	225.1	—	43.03	—	—
B25-F1	267.8	19%	38.63	11.4%	%33
B25-F2	283.2	25.8%	31.2	38.7%	%66
B25-F3	290.1	28.8%	29.58	45.4%	%100

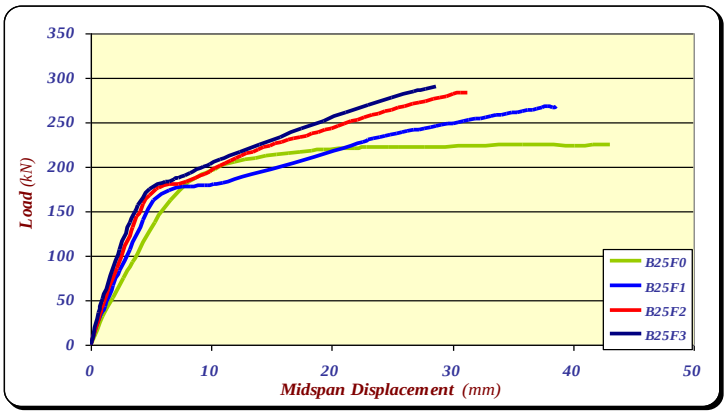

Fig. 11. Load-deflection curves of B25-F group.

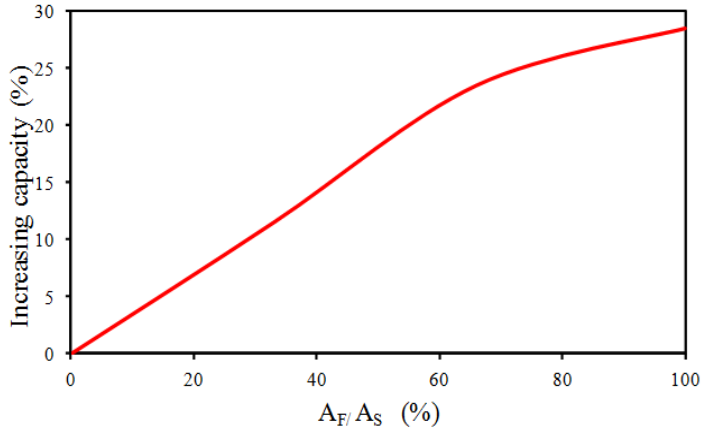

Fig. 20. Effect of cross-area of FRP bars on specimen capacity for F'c=25 MPa

7. Conclusions

To appraise the effectiveness of NSM strengthening technique applied to the flexural strengthening of concrete fixed-support beams, some experimental tests and numerical works were independently carried out. The following conclusions can be drawn from the outcomes of this experimental and numerical research:

- With Strengthening of beams with NSM CFRP bar, stiffness and ultimate strength were increased and also ductility of the specimen was decreased.
- Before the yielding point of the tensile reinforcements, the load-deflection behavior of all beams was similar, so applying NSM FRP reinforcements improve the stiffness of specimen in the plastic range.
- Since A_F in the experimental specimen was less than FRP balance cross-section, so stress in FRP bar increased rapidly and ruptured.
- Numerical load-deflection curve was more stiffness than experimental results due to the higher degrees of nods in experimental compared to numerical.
- The proposed man-made CFRP bars is feasible, easy to apply, and effective in strengthening concrete beams and increased the ultimate load-carrying amount of capacity and improved overall behavior of strengthened beams.
- The strengthening of the fixed-end beam with cylinder compressive strength of 45 MPa consisting of one, two or three FRP bars in each tension zone increased load capacity about 11.5, 23.5% and 28% and decreased mid-span deflection about 5.7, 14.4 and 19.5% respectively .
- The strengthening of the fixed-end beam with cylinder compressive strength of 25 MPa with one, two or three FRP bars in each tension zone increased load capacity about 19, 25.8% and 28.8% and decreased mid-span deflection about 11.4, 38.7 and 45.4% respectively.
- Decreasing of concrete compression strength had the same decreasing effect capacity but the different effect of increasing of deflection at the

various specimen with different FRP area.

REFERENCES

[1] Barros, JAO., Dias, S. (2003). "Shear strengthening of reinforced concrete beams with laminate strips of CFRP." Cosenza (Italy), pp. 289–94.

[2] De Lorenzis, L., Teng, G. J. (2007) "Near Surface Mounted FRP Reinforcement: An Emerging Technique for Strengthening Structures." Composites Part B: Engineering, No. 38, pp. 119-143.

[3] Asplund, S.O. "Strengthening Bridge Slabs with Grouted Reinforcement.", ACI Structure Journal, Vol. 45, Issue 1, pp. 397-406.

[4] Nordin, H., Täljsten, B. (2006). "Concrete Beams Strengthened with Prestressed Near Surface Mounted CFRP." journal of composites for construction, ASCE January.

[5] De Lorenzis, L., Nanni, A., La Tegola, A. (2000). "Flexural and shear strengthening of reinforced concrete structures with near surface mounted FRP rods." In: Proceedings ACMBS III, Ottawa (Canada).

[6] Hassan, T., Rizkalla, S. (2002). ''Flexural strengthening of prestressed bridge slabs with FRP systems.'' PCI J., 47, 76–93.

[7] De Lorenzis, L., Nanni, A. (2002). "Bond between NSM fiber-reinforced polymer rods and concrete in structural strengthening." ACI Structure Journal, 99(2):123–32.

[8] Carolin, A., Hordin, H., Taljsten, B. (2001) "Concrete Beams Strengthened with Near Surface Mounted Reinforcement of CFRP." Proceeding of the International Conference on FRP Composite in Civil Engineering, CICE, Hong Kong, China, Dec 12-15, Vol. 2.

[9] Jalali, M., Sharbatdar, M. Kazem., Jian-Fei, Chen., Farshid Jandaghi Alaee. (2012). "Shear strengthening of RC beams using innovative manually made NSM FRP bars." Construction and Building Materials, Volume 36, Pages 990-1000.

[10] Tanarslan, H.M. (2011). "The effects of NSM CFRP reinforcements for improving the shear capacity of RC beams." Construction and Building Materials, Volume 25, Issue 5, Pages 2663-2673.

[11] Matteo, Breveglieri., Barros, JAO., Gláucia, M., Alessandra, Aprile. (2012). "A parametric study on the effectiveness of the NSM technique for the flexural strengthening of continuous RC slabs." Composites Part B: Engineering, Volume 43, Issue 4, Pages 1970-1987.

[12] Mohammadian, M. (2010) "The Investigation of Flexural Behavior of RC Fixed-End Beams Strengthened with FRP Bars at NSM Method." MS Thesis, Department of Civil Engineering, University of Takestan, Iran.